

Unravelling the role of dopants in the electrocatalytic activity of ceria towards CO₂ reduction in Solid Oxide Electrolysis Cells

Elena Marzia Sala, Nicola Mazzanti, Francesco M. Chiabrera[†], Simone Sanna[§], Mogens B.

Mogensen, Peter V. Hendriksen, Zhongtao Ma, Søren B. Simonsen, Christodoulos

*Chatzichristodoulou**

Department of Energy Conversion and Storage, Technical University of Denmark, Fysikvej,
Building 310, DK-2800, Kgs. Lyngby, Denmark.

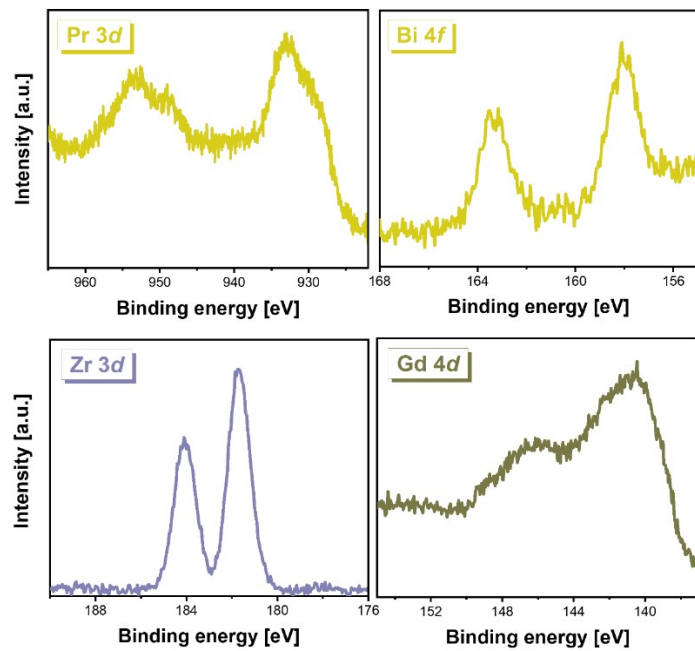


Figure S1. Pr 3d and Bi 4f spectra, Zr 3d spectrum and Gd 4d spectrum measured by XPS on the CPBO, CZO and CGO samples, respectively.

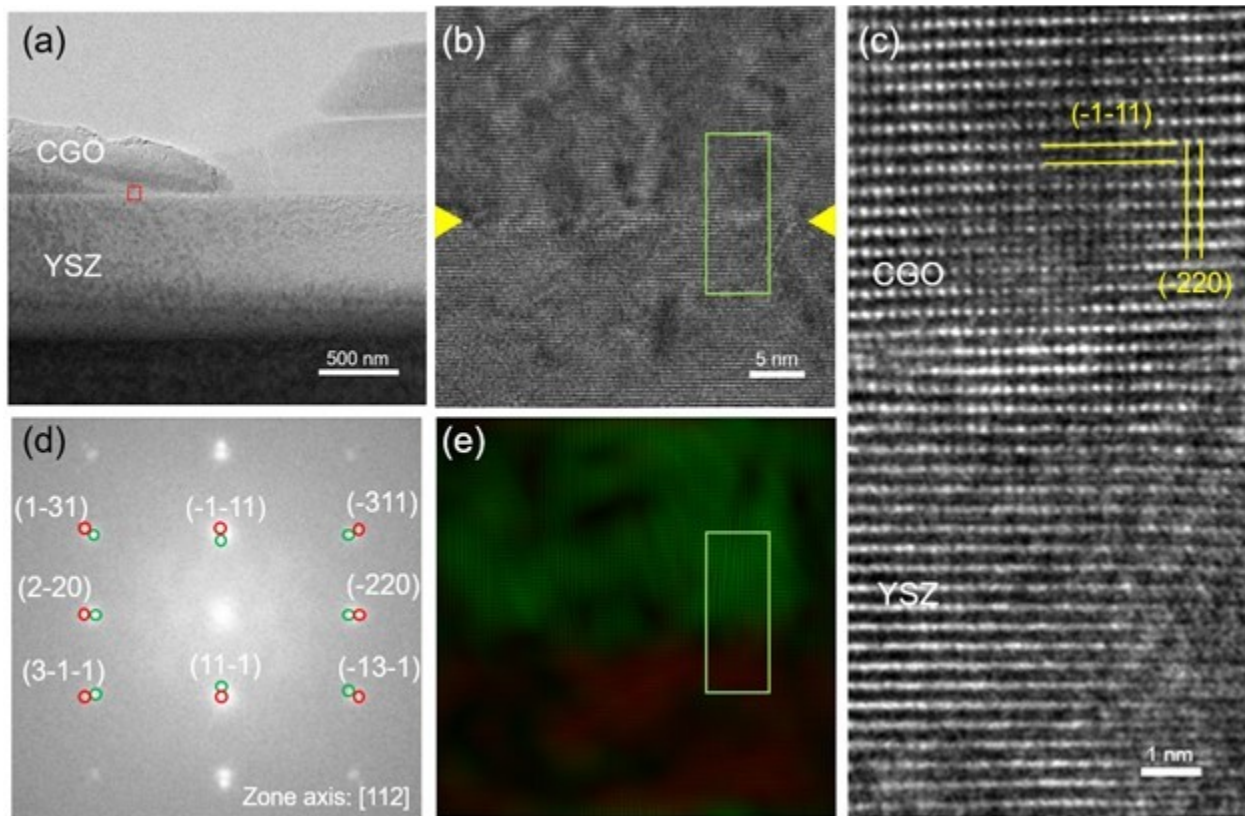


Figure S2. **a** TEM image of a cross section of one CGO sample. **b** HRTEM image of the interface region shown in **a**. To guide the eye, yellow arrows indicate the interface. **c** Close-up of the region indicated with green rectangle in **b** and **e**. **d** FFT of **b**. Lattice planes for low miller indices are identified. The indicated spots belong to CGO (green) and YSZ (red). **e** Inversed FFT of regions indicated with green and red circles in **d**.

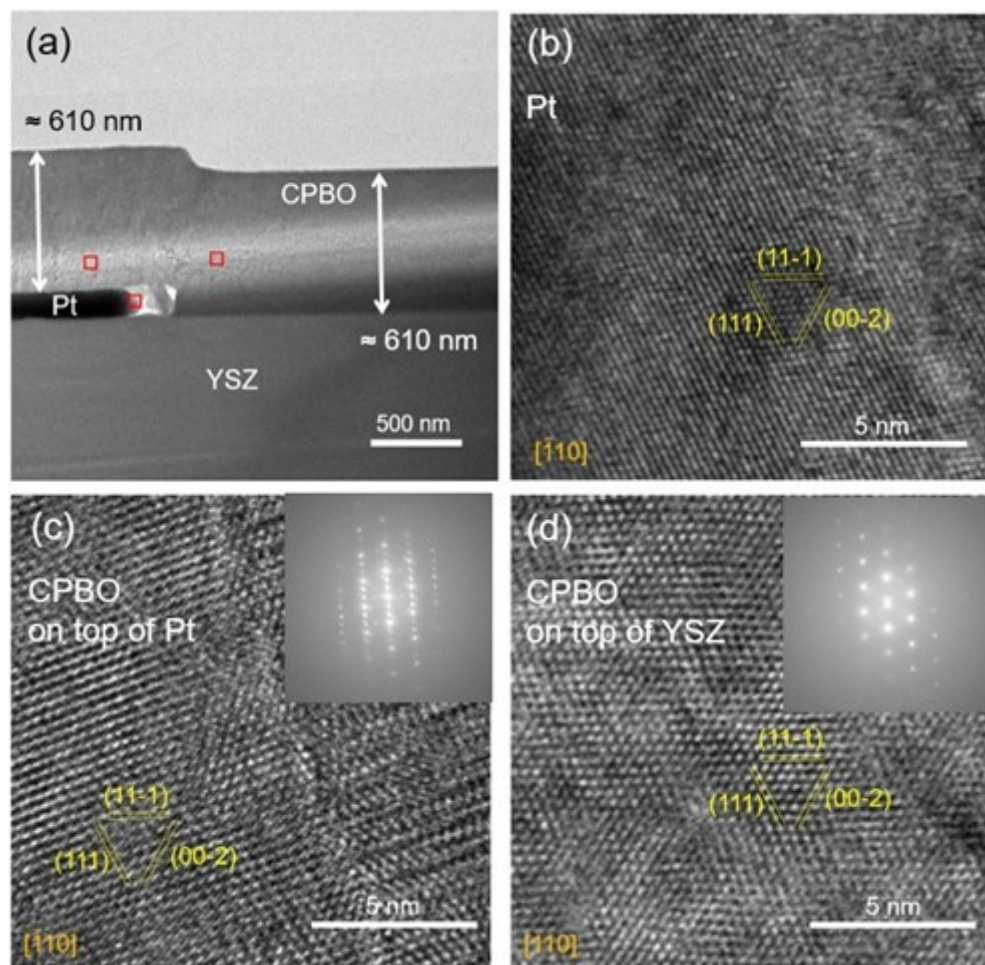


Figure S3. **a** TEM image of a cross section of one CPBO sample. **b** HRTEM image of the red rectangle region over the Pt grid shown in **a**. **c** HRTEM image with corresponding FFT of the red rectangle region of the CPBO film over the Pt grid shown in **a**. **d** HRTEM image with corresponding FFT of the red rectangle region of the CPBO film over the YSZ single crystal shown in **a**.

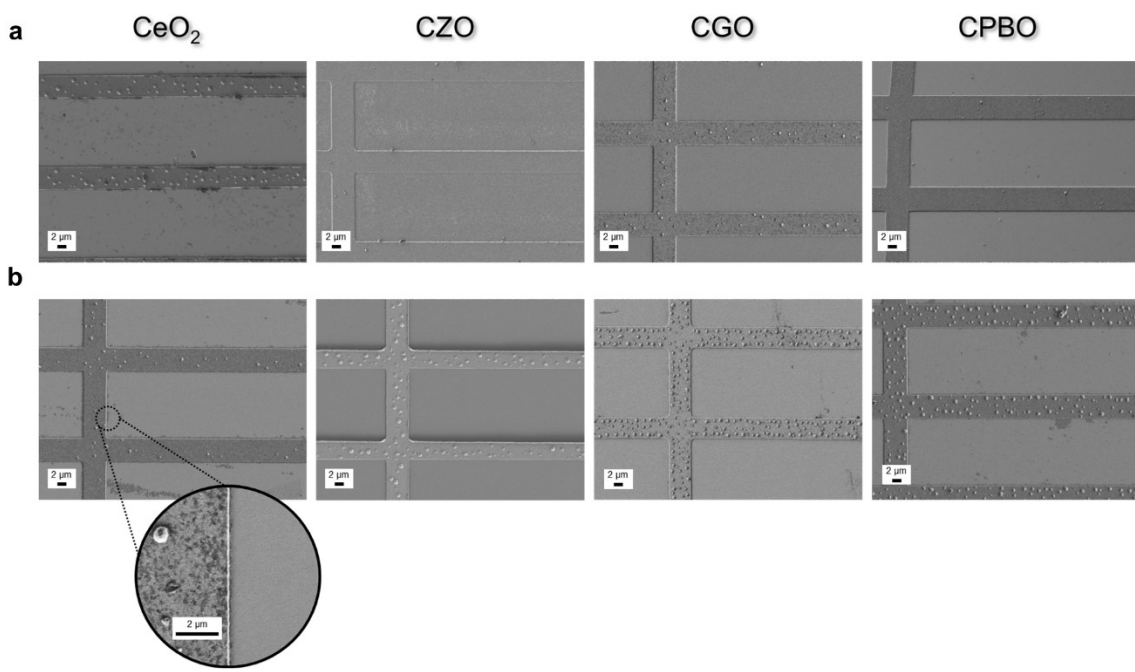
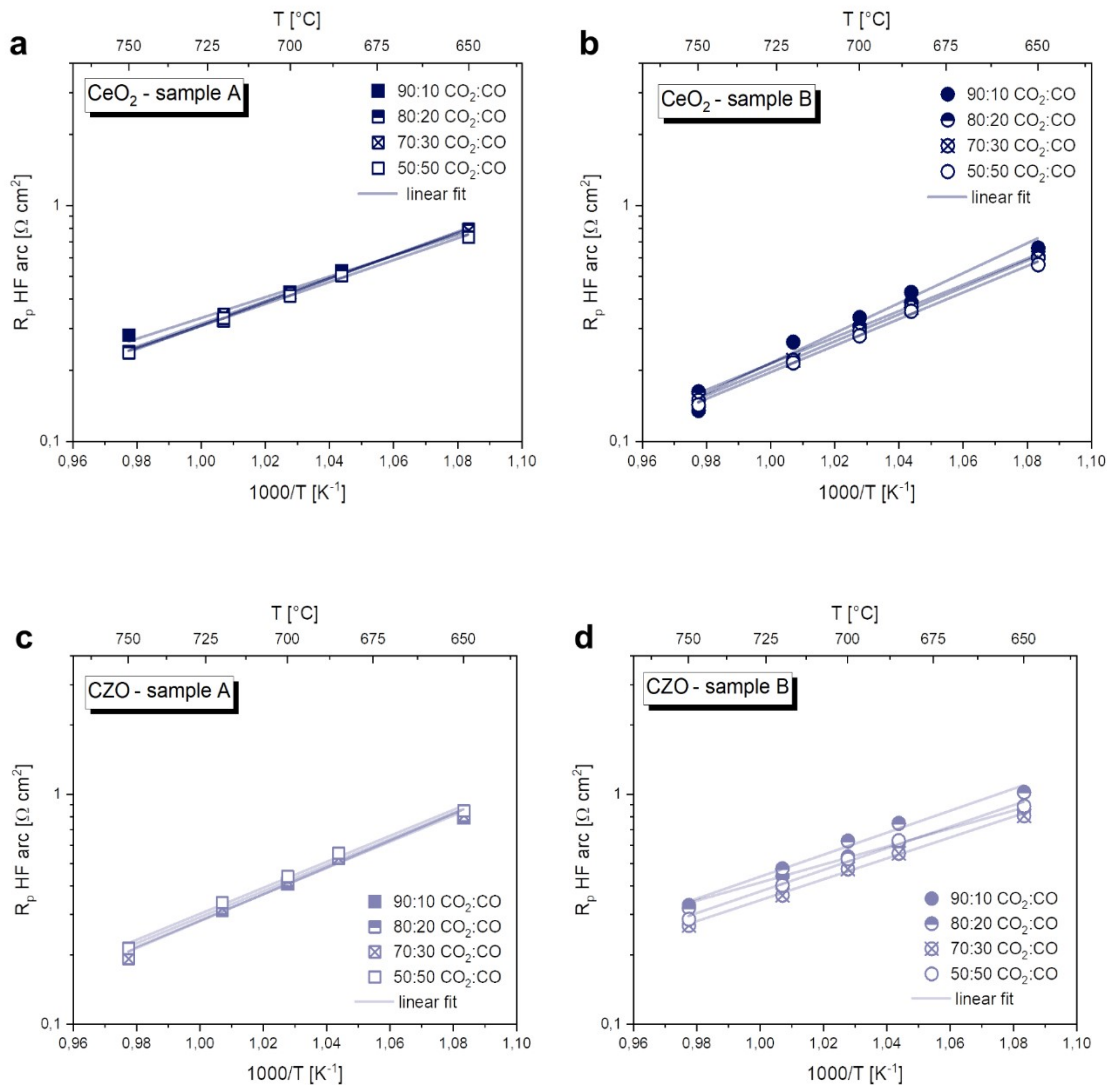


Figure S4. SEM images of the top view of the ceria thin films with different doping composition for **a** the as-deposited samples and **b** after the electrochemical testing. The inset shows the different microstructure of the portion of film grown epitaxial to the substrate with respect to the part grown on the Pt grid.



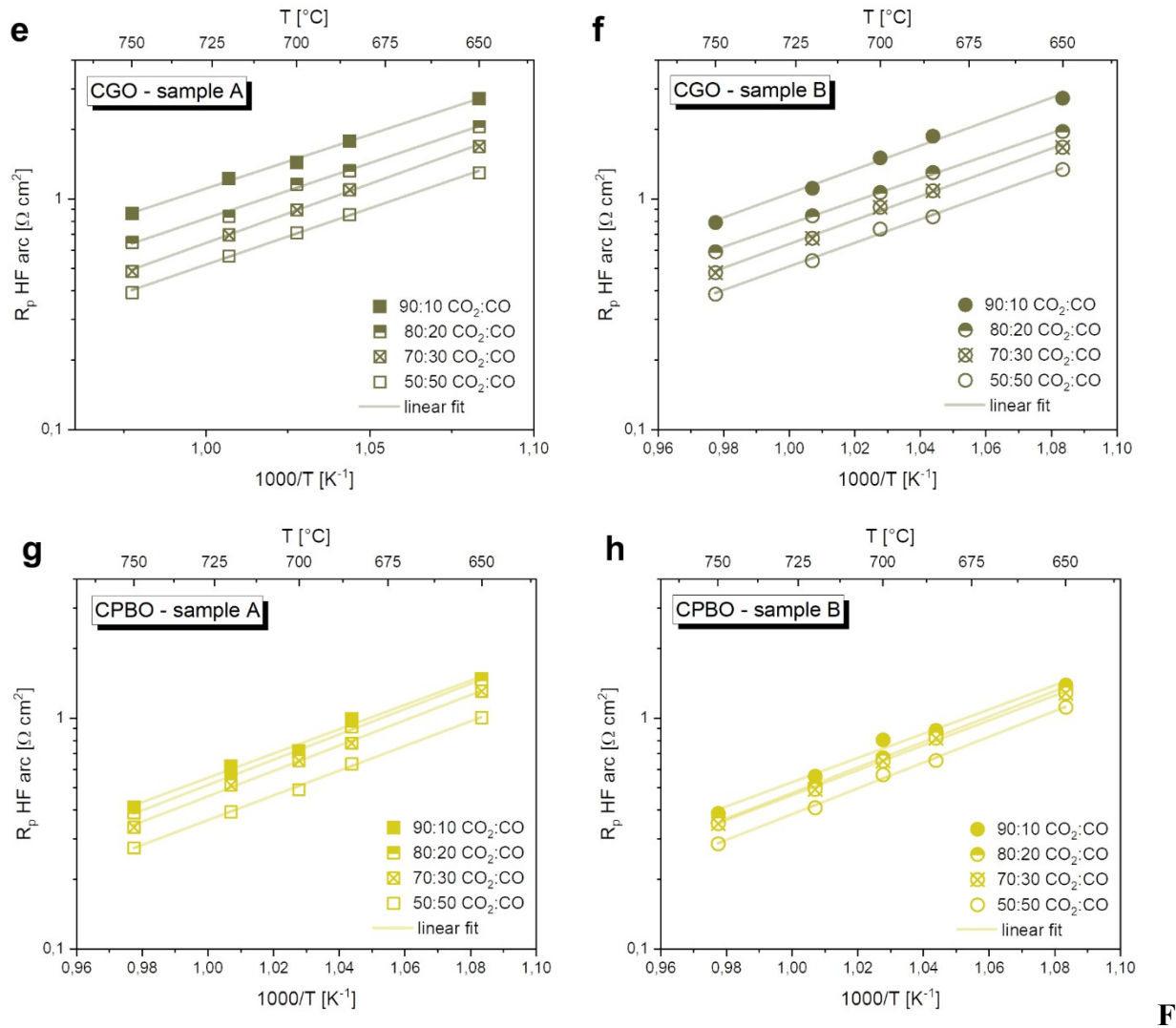


Figure S5. Polarization resistance as a function of temperature of the high frequency contribution for **a, b** CeO₂, **c, d** CZO, **e, f** CGO and **g, h** CPBO. The EIS were recorded at OCV in the temperature range between 650 and 750 °C in varying gas feed mixtures.

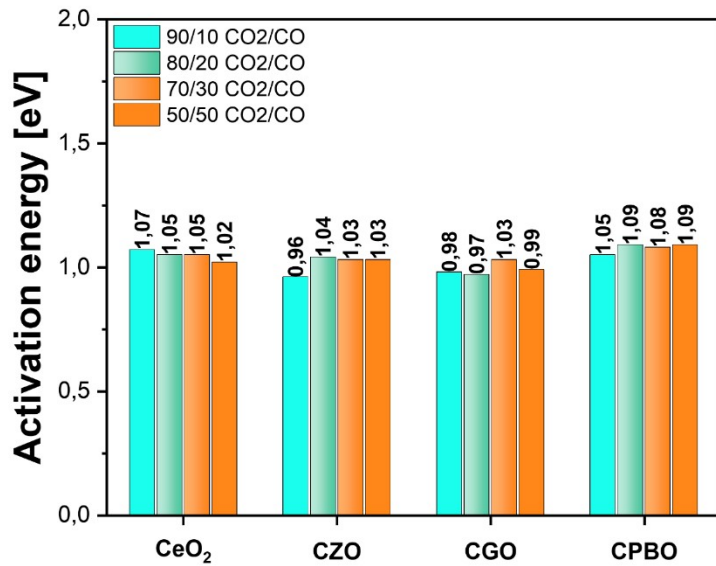


Figure S6. Activation energies of the polarization resistances of the HF arc in the temperature range of 650-750 °C for the 4 different electrode compositions in the gas mixtures investigated at OCV. The values are the average of the electrochemical performance of two identical samples for each doping type. Uncertainties fall within ± 0.1 eV for the all the samples analyzed.

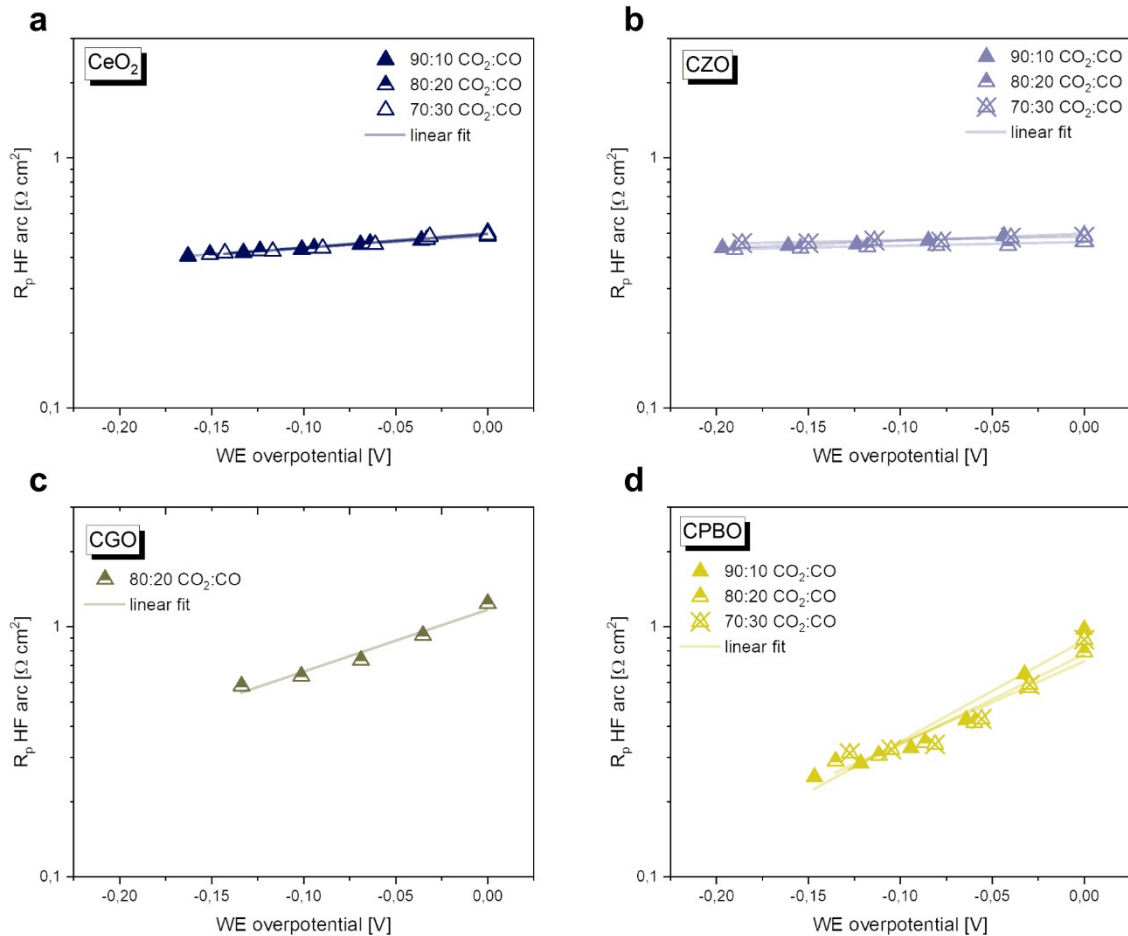


Figure S7. Polarization resistance of the HF arc as a function of the WE overpotential in different gas mixtures for one representative sample of **a** CeO₂, **b** CZO, **c** CGO and **d** CPBO. For CGO only the measurements in 80:20 CO₂:CO are shown due to a set-up malfunctioning that impeded the recording of part of the data.

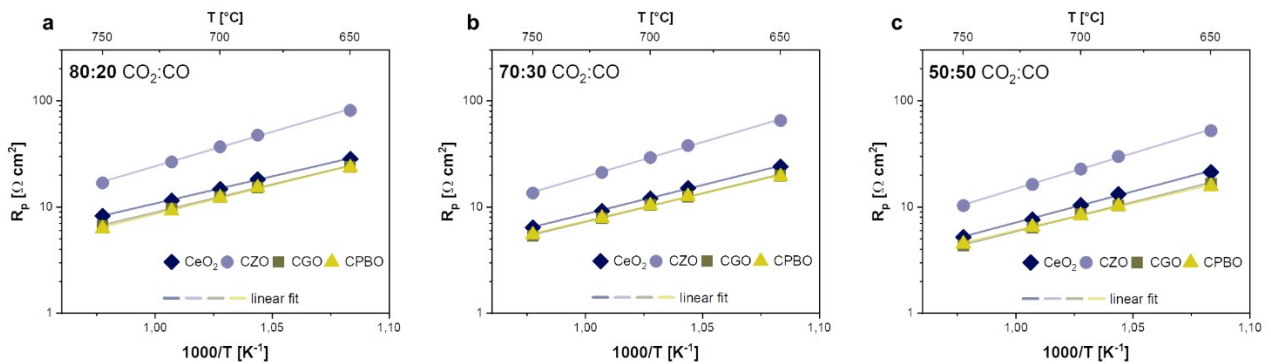


Figure S8. Polarization resistance as a function of temperature at OCV for electrochemical cells with different WE doping type in **a** 80:20 CO₂:CO, **b** 70:30 CO₂:CO and **c** 50:50 CO₂:CO. The values are the average of the electrochemical performance of two identical samples for each doping type.

Note S1. At each step of applied cathodic polarization, the samples were left equilibrating at the desired potential for 10 minutes while carrying out a chronoamperometry (CA) measurement. This ensured that the steady state was reached before measuring the impedance. From the values of current (I_{DC}) flowing between the two electrodes at each given polarization (V_{DC}) measured in the CA routine, the overpotential at the working electrode η could be calculated by subtracting the ohmic loss in the electrolyte ($I_{DC} \cdot R_s$), according to **Eq. S1**:

$$\eta = V_{DC} - I_{DC} \cdot R_s \quad \text{Eq. S1}$$

Table S1: List of possible combinations of the stoichiometric coefficients and associated values

$$of \frac{\partial \log j}{\partial \log pO_2} \Big|_{T,\eta}$$

Sol. nr.	$\nu_{O,1}$	$\nu_{O,2}$	$\nu_{O,3}$	$\nu_{V,1}$	$\nu_{V,2}$	$\nu_{V,3}$	$\nu_{e,1}$	$\nu_{e,2}$	$\nu_{e,3}$	$\frac{\partial \log j}{\partial \log pO_2} \Big _{T,\eta}$
1	0	0	0	0	0	1	0	0	2	0
2	0	0	0	0	0	1	0	1	1	-0.05555555555556
3	0	0	0	0	0	1	0	2	0	-0.11111111111111
4	0	0	0	0	0	1	1	0	1	-0.11111111111111
5	0	0	0	0	0	1	1	1	0	-0.16666666666667
6	0	0	0	0	0	1	2	0	0	-0.22222222222222
7	0	0	0	0	1	0	0	0	2	-0.027777777777778
8	0	0	0	0	1	0	0	1	1	-0.083333333333333
9	0	0	0	0	1	0	0	2	0	-0.138888888888889
10	0	0	0	0	1	0	1	0	1	-0.138888888888889
11	0	0	0	0	1	0	1	1	0	-0.194444444444444
12	0	0	0	0	1	0	2	0	0	-0.25
13	0	0	0	1	0	0	0	0	2	-0.027777777777778
14	0	0	0	1	0	0	0	1	1	-0.083333333333333
15	0	0	0	1	0	0	0	2	0	-0.138888888888889
16	0	0	0	1	0	0	1	0	1	-0.138888888888889
17	0	0	0	1	0	0	1	1	0	-0.194444444444444
18	0	0	0	1	0	0	2	0	0	-0.25
19	0	0	1	0	0	1	0	0	2	0
20	0	0	1	0	0	1	0	1	1	-0.05555555555556
21	0	0	1	0	0	1	0	2	0	-0.11111111111111
22	0	0	1	0	0	1	1	0	1	-0.11111111111111
23	0	0	1	0	0	1	1	1	0	-0.16666666666667
24	0	0	1	0	0	1	2	0	0	-0.22222222222222
25	0	0	1	0	1	0	0	0	2	-0.027777777777778
26	0	0	1	0	1	0	0	1	1	-0.083333333333333
27	0	0	1	0	1	0	0	2	0	-0.138888888888889
28	0	0	1	0	1	0	1	0	1	-0.138888888888889
29	0	0	1	0	1	0	1	1	0	-0.194444444444444
30	0	0	1	0	1	0	2	0	0	-0.25
31	0	0	1	1	0	0	0	0	2	-0.027777777777778
32	0	0	1	1	0	0	0	1	1	-0.083333333333333
33	0	0	1	1	0	0	0	2	0	-0.138888888888889
34	0	0	1	1	0	0	1	0	1	-0.138888888888889
35	0	0	1	1	0	0	1	1	0	-0.194444444444444

36	0	0	1	1	0	0	2	0	0	-0.25
37	0	1	0	0	0	1	0	0	2	0.0277777777777778
38	0	1	0	0	0	1	0	1	1	-0.0277777777777778
39	0	1	0	0	0	1	0	2	0	-0.083333333333333
40	0	1	0	0	0	1	1	0	1	-0.083333333333333
41	0	1	0	0	0	1	1	1	0	-0.138888888888889
42	0	1	0	0	0	1	2	0	0	-0.194444444444444
43	0	1	0	0	1	0	0	0	2	0
44	0	1	0	0	1	0	0	1	1	-0.055555555555556
45	0	1	0	0	1	0	0	2	0	-0.111111111111111
46	0	1	0	0	1	0	1	0	1	-0.111111111111111
47	0	1	0	0	1	0	1	1	0	-0.166666666666667
48	0	1	0	0	1	0	2	0	0	-0.222222222222222
49	0	1	0	1	0	0	0	0	2	0
50	0	1	0	1	0	0	0	1	1	-0.055555555555556
51	0	1	0	1	0	0	0	2	0	-0.111111111111111
52	0	1	0	1	0	0	1	0	1	-0.111111111111111
53	0	1	0	1	0	0	1	1	0	-0.166666666666667
54	0	1	0	1	0	0	2	0	0	-0.222222222222222
55	1	0	0	0	0	1	0	0	2	0.0277777777777778
56	1	0	0	0	0	1	0	1	1	-0.0277777777777778
57	1	0	0	0	0	1	0	2	0	-0.083333333333333
58	1	0	0	0	0	1	1	0	1	-0.083333333333333
59	1	0	0	0	0	1	1	1	0	-0.138888888888889
60	1	0	0	0	0	1	2	0	0	-0.194444444444444
61	1	0	0	0	1	0	0	0	2	0
62	1	0	0	0	1	0	0	1	1	-0.055555555555556
63	1	0	0	0	1	0	0	2	0	-0.111111111111111
64	1	0	0	0	1	0	1	0	1	-0.111111111111111
65	1	0	0	0	1	0	1	1	0	-0.166666666666667
66	1	0	0	0	1	0	2	0	0	-0.222222222222222
67	1	0	0	1	0	0	0	0	2	0
68	1	0	0	1	0	0	0	1	1	-0.055555555555556
69	1	0	0	1	0	0	0	2	0	-0.111111111111111
70	1	0	0	1	0	0	1	0	1	-0.111111111111111
71	1	0	0	1	0	0	1	1	0	-0.166666666666667
72	1	0	0	1	0	0	2	0	0	-0.222222222222222